$J/\psi+\gamma$ production at the CERN LHC

Prakash Mathews* and K. Sridhar†
Department of Theoretical Physics, Tata Institute of Fundamental Research, Homi Bhabha Road, Bombay 400 005, India

Rahul Basu‡
Institute of Mathematical Sciences, CPT Campus, Chennai 600 113, India

(Received 21 January 1999; published 3 June 1999)

The associated production of $J/\psi+\gamma$ at the CERN LHC is studied within the NRQCD framework. The signal we focus on is the production of a J/ψ and an isolated photon produced back to back, with their transverse momenta balanced. It is shown that even for very large values of transverse momentum ($p_T \sim 50$ GeV) the dominant contribution to this process is *not* fragmentation. This is because of the fact that fragmentation-type contributions to the cross section come from only a $q\bar{q}$ initial state, which is suppressed at the LHC. We identify gg-initiated diagrams higher-order in α_s which do have fragmentation-type vertices. We find, however, that the contribution of these diagrams is negligibly small. [S0556-2821(99)03613-9]

PACS number(s): 13.85.Ni, 13.85.Qk

Nonrelativistic QCD (NRQCD) is an effective field theory derived from the full QCD Lagrangian by neglecting all states of momenta larger than a cutoff of the order of the heavy quark mass, m [1], and accounting for this exclusion by introducing new interactions in the effective Lagrangian, which are local since the excluded states are relativistic. It is then possible to expand the quarkonium state in terms of its Fock components as a perturbation series in v (where v is the relative velocity between the heavy quarks), and in this expansion, the $Q\bar{Q}$ states appear in either color-singlet or color-octet configurations. The color-octet $Q\bar{Q}$ state is connected to the physical state by the emission of one or more soft gluons by transitions which are dominantly non-spin-flip and spin-flip transitions. Selection rules for these radiative transitions then allow us to keep track of the quantum numbers of the octet states, so that the production of a $Q\bar{Q}$ pair in a octet state can be calculated and its transition to a physical singlet state can be specified by a non-perturbative matrix element. The cross section for the production of a meson H then takes on the following factorized form:

$$\sigma(H)=\sum_{n=\{\alpha,S,L,J\}}\frac{F_n}{m^{d_n-4}}\langle\mathcal{O}_\alpha^H({}^{2S+1}L_J)\rangle \qquad (1)$$

where F_n's are the short-distance coefficients and $\mathcal{O}_n$ are local 4-fermion operators, of naive dimension d_n, describing the long-distance physics. The short-distance coefficients are associated with the production of a $Q\bar{Q}$ pair with the color and angular momentum quantum numbers indexed by n. These involve momenta of the order of m or larger and can be calculated in a perturbation expansion in the coupling $\alpha_s(m)$. The non-perturbative long-distance factor $\langle O_n^H\rangle$ is proportional to the probability for a pointlike $Q\bar{Q}$ pair in the state n to form a bound state H. These matrix elements are universal in the sense that having extracted them in a particular process, they can be used to make predictions for other processes involving quarkonia.

In fact, the importance of the color-octet components was first noted [2] in the case of P-wave charmonium decays, and even in the production case the importance of these components was first seen [3,4] in the production of P-state charmonia at the Tevatron. The surprise was that even for the production of S states such as the J/ψ or ψ', where the color singlet components give the leading contribution in v, the inclusion of sub-leading octet states was seen to be necessary for phenomenological reasons [5]. While the inclusion of the color-octet components seems to be necessitated by the Tevatron charmonium data, the normalization of these data cannot be predicted because the long-distance matrix elements are not calculable. The data allow a linear combination of octet matrix elements to be fixed [6,7], and much effort has been made recently to understand the implications of these color-octet channels for J/ψ production in other processes: for example, J/ψ production at the CERN e^+e^- collider LEP [8,9], the prediction for the polarization of the J/ψ [10], production of J/ψ at fixed-target pp and πp experiments [11], inelastic photoproduction at the DESY ep collider HERA [12–14], production of quarkonium states at the CERN Large Hadron Collider (LHC) [15] and the predictions for the large-p_T production of other charmonium resonances at the Fermilab Tevatron [16]. Recently, next-to-leading order calculations for quarkonium production at low p_T have also been completed [17] and make it possible to make accurate predictions for these processes.

In this paper we consider the large p_T associated production of an isolated photon and J/ψ produced back to back at LHC energies. This process was first studied [18] in the context of the color-singlet model, and more recently, the contribution of the color-octet channels at the Tevatron has also been studied [19,20]. The tree-level cross section for the $J/\psi+\gamma$ process can be obtained from the corresponding cross sections for the photoproduction of J/ψ which have

*Email address: prakash@theory.tifr.res.in
†Email address: sridhar@theory.tifr.res.in
‡Email address: rahul@imsc.ernet.in

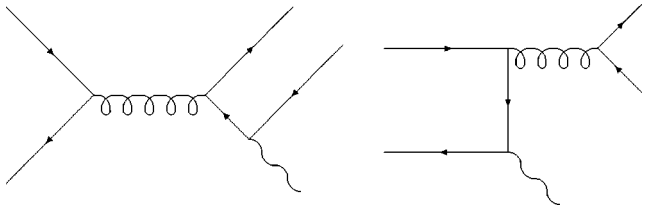

FIG. 1. Quark tree diagrams.

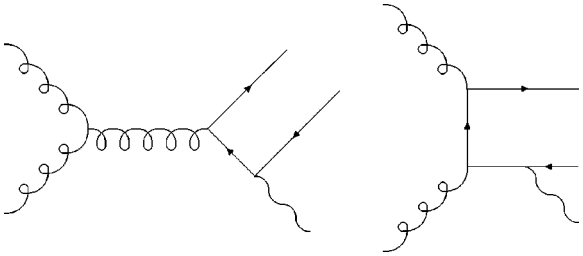

FIG. 2. Gluon tree diagrams.

been calculated in Ref. [12]. It turns out that, because of the photon in the final state, the color-singlet contribution is more important for this process than for inclusive J/ψ production at the Tevatron. In fact, this process can be a sensitive probe of quarkonium production and it is our aim, in the present work, to understand how it may be used to unravel aspects of quarkonium production dynamics at the LHC.

The contributing subprocesses to $J/\psi+\gamma$ production are

$$q\bar{q}\rightarrow {}^{2S+1}L_J\gamma,$$
$$gg\rightarrow {}^{2S+1}L_J\gamma. \tag{2}$$

The Fock components that contribute to J/ψ production are the color-singlet ${}^3S_1^{[1]}$ state and the color-octet states ${}^3S_1^{[8]}$, ${}^1S_0^{[8]}$ and ${}^3P_{0,1,2}^{[8]}$. The color-singlet ${}^3S_1$ state contributes at $\mathcal{O}(1)$ but the color-octet channels all contribute higher orders in v. This is because the ${}^3S_1^{[8]}$ connects to the J/ψ by emitting two soft gluons [both non-spin-flip transitions and resulting in an effective $\mathcal{O}(v^4)$ suppression] while the ${}^1S_0^{[8]}$ connects to the physical state via a spin-flip transition [the correct power counting for which yields an effective $\mathcal{O}(v^3)$ suppression[1]]. On the other hand, the ${}^3P_{0,1,2}^{[8]}$ states connect to the J/ψ by a single non spin-flip transition but since they are $L=1$ states their production cross section is already suppressed by $\mathcal{O}(v^2)$, making them effectively of $\mathcal{O}(v^4)$.

In the α_s perturbation series, we will first study all contributions to $\mathcal{O}(\alpha\alpha_s^2)$, i.e. the tree-level diagrams, and then we will study the effect of a class of higher-order (in α_s) diagrams which are likely to be important for the process under consideration. The net contribution of the various subprocess depends on various factors:

(i) the initial parton flux,

(ii) the order in v of the final contributing non-perturbative NRQCD matrix element, and

(iii) the p_T behavior of the subprocess.

In Figs. 1 and 2, we have shown some examples of tree-level contributions to this process. From our experience with large-p_T J/ψ production at the Tevatron, one gleans the fact that it is expedient to classify these diagrams in terms of the number of heavy-quark propagators in them. To this end we introduce some notation: the diagrams where only one gauge boson attaches itself to the $Q\bar{Q}$ pair is called a one-vertex or 1V diagram. Such diagrams have no heavy-quark propagators and are fragmentation-like diagrams. Similarly there are two-vertex (2V) and three-vertex (3V) diagrams, which have one and two heavy quark propagators, respectively. This classification is useful in understanding the systematics of J/ψ production at large p_T at the Tevatron. In the case of inclusive production, it turns out that the 1V diagrams (which are fragmentation like) are those that dominate at large p_T. It is straightforward to convince oneself (by using the spin and color projectors used in quarkonium calculations) that the only state that can be produced in a 1V diagram is the ${}^3S_1^{[8]}$ state. Consequently, J/ψ production at large p_T is completely dominated by ${}^3S_1^{[8]}$ production [7]. On the other hand, at the lower end of the p_T spectrum at the Tevatron, there is a significant contribution from the ${}^1S_0^{[8]}$ and ${}^3P_{0,1,2}^{[8]}$ states. These come from 2V diagrams with the contribution from the 3V diagrams being less important. In fact, it is this p_T dependence that allows for a separate determination of the $\langle {}^3S_1^{[8]}\rangle$ matrix element. On the other hand, it is not possible to determine the $\langle {}^1S_0^{[8]}\rangle$ and $\langle {}^3P_{0,1,2}^{[8]}\rangle$ matrix elements separately because they have a similar p_T dependence owing to the fact that the production of these states proceeds dominantly via 2V diagrams.

At the LHC, the situation is somewhat different. At the large energies and large p_T values that will be available at the LHC, the production of J/ψ is expected to be overwhelmed by the intermediate production of a ${}^3S_1^{[8]}$ state. The contribution of the ${}^1S_0^{[8]}$ and ${}^3P_{0,1,2}^{[8]}$ states is very small [15]. The complete dominance of the fragmentation-type contributions for J/ψ production at the LHC is also because of the fact that the production mechanisms in LHC which dominate are gg initiated. This is an important point to keep in mind when we study $J/\psi+\gamma$ production, because if we consider the tree diagrams for this process, we find that there is no 1V diagram contributing through a gg-initiated channel. The only 1V diagram that contributes is in the $q\bar{q}$-initiated channel. Consequently, we expect that fragmentation-type subprocesses are not as important to this process as they are for the case of J/ψ production.

To check out these expectations, we have studied the production of $J/\psi+\gamma$ at the LHC ($\sqrt{s}=14$ TeV). In Fig. 3, we present the results for the cross section $Bd\sigma/dp_T$ as a function of p_T. We have assumed $-2.5<y<2.5$ in our computations. For the input parton distributions, we use the Martin-Roberts-Stirling set D-$'$ (MRSD-$'$) [21] and evolved them to the scale $Q=M_T$. For the numerical values of the relevant non-perturbative matrix elements we use the numbers tabulated below which have been obtained [7] by fitting to the Collider Detector at Fermilab (CDF) data. We would like to point out here that the inclusion of soft-gluon radiation ef-

[1]See the erratum of Ref. [1].

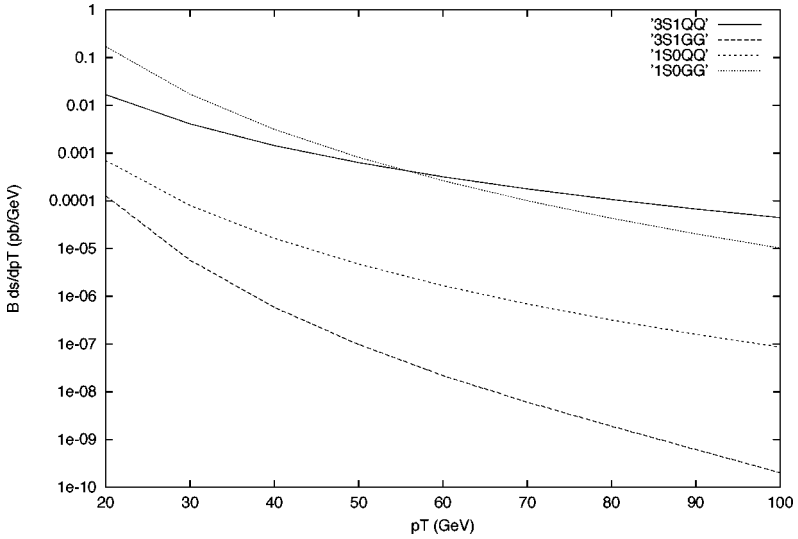

FIG. 3. $Bd\sigma/dp_T$ for $J/\psi+\gamma$ production at the LHC.

fects [22,23,14] leads to lower fitted values for the nonperturbative parameters, but these effects are somewhat model dependent. For the purposes of the present analysis, we prefer to use the matrix elements derived by Ref. [7]:

$$\langle \mathcal{O}_1^{J/\psi}(^3S_1)\rangle = 1.2 \ \text{GeV}^3,$$

$$\langle \mathcal{O}_8^{J/\psi}(^3S_1)\rangle = (6.6\pm 2.1)\times 10^{-3} \ \text{GeV}^3,$$

$$\frac{\langle \mathcal{O}_8^{J/\psi}(^3P_0)\rangle}{M_c^2} + \frac{\langle \mathcal{O}_8^{J/\psi}(^1S_0)\rangle}{3} = (2.2\pm 0.5)\times 10^{-2} \ \text{GeV}^3. \tag{3}$$

Since only the sum of $\langle {}^1S_0^{[8]}\rangle$ and $\langle {}^3P_0^{[8]}\rangle$ matrix elements can be extracted from the J/ψ CDF data, we make prediction by considering the maximal case, i.e., saturating the sum by either the ${}^1S_0^{[8]}$ or ${}^3P_0^{[8]}$ matrix elements. Using heavy quark spin symmetry the other matrix elements are related: $\langle \mathcal{O}_8^{J/\psi}(^3P_J)\rangle = (2J+1)\langle \mathcal{O}_8^{J/\psi}(^3P_0)\rangle$. First let us consider the case in which the $\langle {}^1S_0^{[8]}\rangle$ saturates the sum in Eq. (3). The contributions would hence come from the ${}^1S_0^{[8]}$ and the ${}^3S_1^{[8]}$ terms. We find that even up to a value of 50 GeV in p_T, the dominant contribution is that which comes from the 2V diagrams involving the ${}^1S_0^{[8]}$ state. This is because of the fact that this subprocess is gg initiated. It is only above a p_T of 50 GeV that the $q\bar{q}$-initiated 1V diagram starts dominating. The upshot of this computation is that at the LHC energies there is an interesting interplay between the initial parton flux and the fragmentation-type effects, and because of the fact that the $q\bar{q}$ flux is small at these energies, the effects of fragmentation do not show up until the p_T values become very large. We have also checked that the results are more or less unchanged even if we saturate the sum in Eq. (3) with the $\langle {}^3P_0^{[8]}\rangle$ matrix element.

It is also important to check whether this is only because we have restricted ourselves to tree-level diagrams. In principle, it is possible that 1V diagrams which are higher order in α_s and which come from a gg initial state could modify this result. In spite of being higher order in α_s, being 1V diagrams, these are possibly enhanced by powers of p_T/m. In the following we identify the possible higher-order diagrams that can contribute and try to estimate the magnitude of these corrections.

Let us consider the possible higher-order diagrams coming from a gg initial state that could contribute to the signal. Since the signal that we demand is a p_T-balanced J/ψ and an isolated photon final state, the only 1V diagrams that we can have are triangle and box diagrams with quark loops. These are shown in Figs. 4 and 5. It can be shown that the contribution of the 1V triangle diagram is zero. The triangle is attached to one photon and two gluons, and vanishes due to Furry's theorem.

The box diagram (shown in Fig. 5) corresponds to the

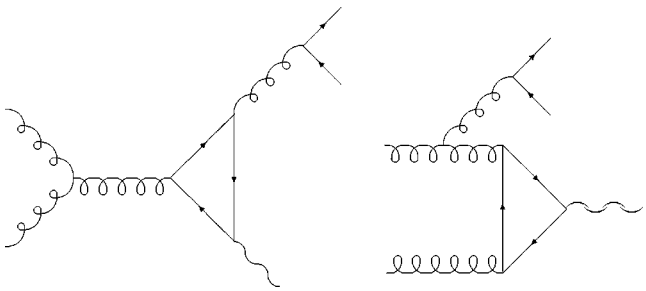

FIG. 4. Fragmentation type triangle diagrams.

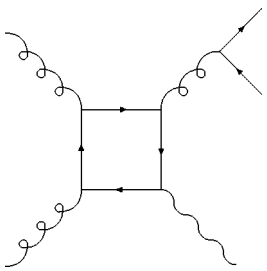

FIG. 5. Box diagram.

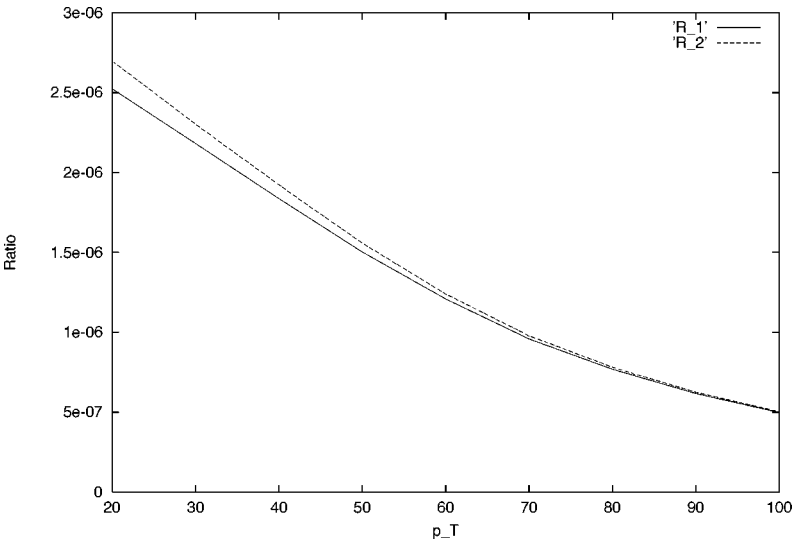

FIG. 6. The ratio R of the box diagram contribution to the tree level cross section, for the two cases described in the text.

process $gg \to g\gamma$ through a quark loop and the outgoing gluon fragmenting into a $Q\overline{Q}$ pair which finally forms a J/ψ through an intermediate $^3S_1^{[8]}$ state. We choose the number of quark flavors in the loop as 4. This diagram has a non-vanishing interference with the tree level $gg \to Q\overline{Q}(^3S_1^{[8]})\gamma$. We begin by evaluating the interference term. The box diagram has three terms (corresponding to the three different ways that the photon can be attached to the internal quark lines) and three terms with the loop momenta reversed. It turns out that the contributions of the latter three diagrams are the same as the former. The individual diagrams are superficially divergent and we use dimensional regularization to regulate it. Feynman parametrization has to be done symmetrically and leads to a lot of simplification. This gives terms proportional to $(L^2)^n$ where L is the loop momenta and $n=0,1,2$. Terms proportional to $n=0,1$ are finite but the $n=2$ term is divergent. It can be shown that on combining all three diagrams, the $1/\epsilon$ pole cancels to give a finite part and a logarithmic term. We have extensively used FORM and MATHEMATICA for the calculation of the interference contribution and used the output of these packages directly for our numerical computations. The results of our computation are shown in Fig. 6, where we have plotted the ratio R of the magnitude of the interference term to the tree level cross section. As before, the results are obtained using MRSD-$'$ densities and a rapidity cut $-2.5<y<2.5$. The two curves R_1 and R_2 shown in Fig. 6 correspond to the two values of the tree-level cross sections obtained from saturating the sum in Eq. (3) with either of the two non-perturbative matrix elements. We find that the contribution of the interference is tiny, and the factors associated with the box diagram suppress any possible enhancement expected from the gluon flux and fragmentation contribution. Given that the interference term is so small, we expect the box amplitude square contribution to be even further suppressed.

In summary, we have studied the associated production of $J/\psi+\gamma$, produced back to back, at the LHC. We find that this process gives us crucial insights into the dynamics of quarkonium production. In particular, we find that production via fragmentation-like diagrams does not dominate the cross section up to values of 50 GeV. This is because of the fact that there is no such contribution in the gg-initiated channel, but only in the $q\overline{q}$-initiated channel, where the corresponding parton flux is small. Beyond the tree level, we find that there is a box diagram with a gg initial state that contributes to this process, but we find the contribution of this diagram to be negligibly small.

The authors wish to thank the organizers of the Fifth Workshop on High Energy Physics Phenomenology (WHEPP-5) held in IUCAA, Pune, India, where this work was initiated.

[1] G. T. Bodwin, E. Braaten, and G. P. Lepage, Phys. Rev. D **51**, 1125 (1995); **55**, 5853(E) (1997).
[2] G. T. Bodwin, E. Braaten, and G. P. Lepage, Phys. Rev. D **46**, R1914 (1992).
[3] F. Abe *et al.*, Phys. Rev. Lett. **71**, 2537 (1993).
[4] E. Braaten, M. A. Doncheski, S. Fleming, and M. Mangano, Phys. Lett. B **333**, 548 (1994); D. P. Roy and K. Sridhar, *ibid.* **339**, 141 (1994); M. Cacciari and M. Greco, Phys. Rev. Lett. **73**, 1586 (1994).
[5] E. Braaten and S. Fleming, Phys. Rev. Lett. **74**, 3327 (1995).
[6] M. Cacciari, M. Greco, M. Mangano, and A. Petrelli, Phys. Lett. B **356**, 553 (1995).
[7] P. Cho and A. K. Leibovich, Phys. Rev. D **53**, 150 (1996); **53**, 6203 (1996).
[8] K. Cheung, W.-Y. Keung, and T. C. Yuan, Phys. Rev. Lett. **76**, 877 (1996); S. Baek, P. Ko, J. Lee, and H. S. Song, Phys. Lett. B **389**, 609 (1996).
[9] P. Cho, Phys. Lett. B **368**, 171 (1996).

[10] P. Cho and M. Wise, Phys. Lett. B **346**, 129 (1995); S. Baek, P. Ko, J. Lee, and H. S. Song, Phys. Rev. D **55**, 6839 (1997); M. Beneke and I. Rothstein, Phys. Lett. B **372**, 157 (1996); M. Beneke and M. Krämer, Phys. Rev. D **55**, 5269 (1997).
[11] S. Gupta and K. Sridhar, Phys. Rev. D **54**, 5545 (1996); M. Beneke and I. Rothstein, *ibid.* **54**, 2005 (1996); S. Gupta and K. Sridhar, *ibid.* **55**, 2650 (1997).
[12] M. Cacciari and M. Krämer, Phys. Rev. Lett. **76**, 4128 (1996); P. Ko, J. Lee, and H. S. Song, Phys. Rev. D **54**, 4312 (1996).
[13] M. Beneke, I. Z. Rothstein, and M. B. Wise, Phys. Lett. B **408**, 373 (1997).
[14] K. Sridhar, A. D. Martin, and W. J. Stirling, Phys. Lett. B **438**, 211 (1998).
[15] K. Sridhar, Mod. Phys. Lett. A **11**, 1555 (1996).
[16] K. Sridhar, Phys. Rev. Lett. **77**, 4880 (1996); P. Mathews, P. Poulose, and K. Sridhar, Phys. Lett. B **438**, 336 (1998).
[17] A. Petrelli *et al.*, Nucl. Phys. **B514**, 215 (1998); F. Maltoni, M. L. Mangano, and A. Petrelli, *ibid.* **B519**, 361 (1998).
[18] M. Drees and C. S. Kim, Z. Phys. C **53**, 673 (1992); K. Sridhar, Phys. Rev. Lett. **70**, 1747 (1993); C. S. Kim and E. Reya, Phys. Lett. B **300**, 298 (1993).
[19] C. S. Kim, J. Lee, and H. S. Song, Phys. Rev. D **55**, 5429 (1997).
[20] D. P. Roy and K. Sridhar, Phys. Lett. B **341**, 413 (1995).
[21] A. D. Martin, R. G. Roberts, and W. J. Stirling, Phys. Lett. B **306**, 145 (1993); **309**, 492 (1993).
[22] B. Cano-Coloma and M. A. Sanchis-Lozano, Nucl. Phys. **B508**, 753 (1997).
[23] B. A. Kniehl and G. Kramer, Eur. Phys. J. C **6**, 493 (1998).